Progress In Electromagnetics Research Letters, Vol. 98, 1–8, 2021

A Dual-Band 8-Element 4/5G Printed MIMO Antenna Using Open Slot Radiators

Mohamed M. Morsy*

Abstract—This paper presents a dual-band eight-element multiple-input multiple-output (MIMO) antenna for 5G applications. The 8-element antenna is formed into two 4×4 MIMO systems that operate at 2500–2600 MHz and 1800–2200 MHz bands. The antenna elements are mounted along the perimeter of a rectangular ground plane with a total size of $110 \times 80\,\text{mm}^2$ and are printed on both sides of a low-profile PCB material. Elements radiate through open rectangular slots etched on the antenna's ground conductor. The open slots are excited by T-shaped microstrip lines fed by 50-Ω coaxial connectors. The size of the ground plane's slots, and the T-shaped radiators control the resonance of the antenna's elements. The proposed design employs orthogonal elements to mitigate mutual coupling. The isolation between ports is less than -10 dB. The radiation efficiency ranges from 40% to 65% across operating frequency bands.

1. INTRODUCTION

The fifth-generation (5G) technology is expected to provide valuable solutions for the current 4G latency problem. 5G communication will unlock the full capacity of internet-of-things (IoT) technology. IoT technology supported with 5G communication will provide high bandwidth, low latency, and high-efficiency IoT systems [1]. 5G spectrum is classified into three main categories sub 1 GHz, 1–6 GHz, and millimetre wave bands. Sub 1 GHz is used for LTE and 5G applications in almost 153 countries. Its coverage includes the 700-MHz (Bands 12, 13, 14, 17, or 28), 800-MHz (Band 20), and 900-MHz (Band 8) frequency bands. Other less popular sub 1 GHz coverages include 450-MHz (Band 31) and 600-MHz (Band 71) [2]. 1–6 GHz offers various coverage including 3.3–3.8 GHz band, which is primarily designated for 5G operation. Other bands, including 1800 MHz, 2300 MHz, and 2600 MHz, are being reassigned for 5G operations as well. For above 6 GHz, millimeter-wave bands at 26 GHz and 28 GHz are commonly used to support ultra-broadband coverage of 5G communications.

MIMO antenna configuration is essential for 4G and 5G communications to achieve a high data rate and enhanced reliability, as shown in [3–15]. Multiple techniques have been used to enhance the radiation properties of MIMO antennas and improve isolation between radiation elements. 5G MIMO antennas require at least four elements as opposed to 4G MIMO antenna, which requires at least two radiating elements. It increases the challenge of designing a compact antenna that can fit in user terminals while maintaining good isolation and radiation performance. Multiple designs are based on radiating through an open slot etched on a ground plane as in [3, 8, 13, 16]. Other antennas employ decoupling structures to mitigate the mutual coupling effect of adjacent elements as in [8, 9]. Recently, a large number of 5G MIMO antennas have employed self-decoupled elements where no decoupling structure is needed, as in [4, 7, 16]. However, the main drawback of the design is the non-planar structure of the design and

Received 24 March 2021, Accepted 19 April 2021, Scheduled 21 April 2021

* Corresponding author: Mohamed M. Morsy (mmorsy@tamut.edu).

The author is with the Electrical Engineering Department, Texas A&M University-Texarkana, 7101 University Ave, Texarkana, TX, USA.

the need for accurate assembly, which can be challenging for mass production. PIFA structures have also been used in 5G models, as in [10].

In this paper, an 8-element MIMO array antenna is presented for 5G applications. The 8-element MIMO array forms two 4×4 MIMO systems operating at 1800–2200 MHz and 2500–2600 MHz, respectively. The proposed antenna employs open slot radiators that are excited using T-shape microstrip lines. Typically, many sub 6-GHz MIMO antennas have been designed to cover both 4G LTE and 5G systems as in [11, 17–19]. Elements are positioned around the perimeter of a rectangular PCB FR4 material of permittivity 4.4 and thickness 0.8 mm. The orthogonal orientation of radiating elements helps mitigate mutual coupling without the need for additional isolation structures. The proposed MIMO antenna is simulated, fabricated, and measured. CST Studio Suite 2021 is used for simulation [20]. The simulated and measured results are in good agreement. Radiation and diversity performances are analysed.

2. ANTENNA DESIGN

The geometry of the proposed 5G MIMO antenna is presented in Figure 1. The parameter values of the proposed MIMO antennas are shown in Table 1. The antenna is printed on FR4 material with a

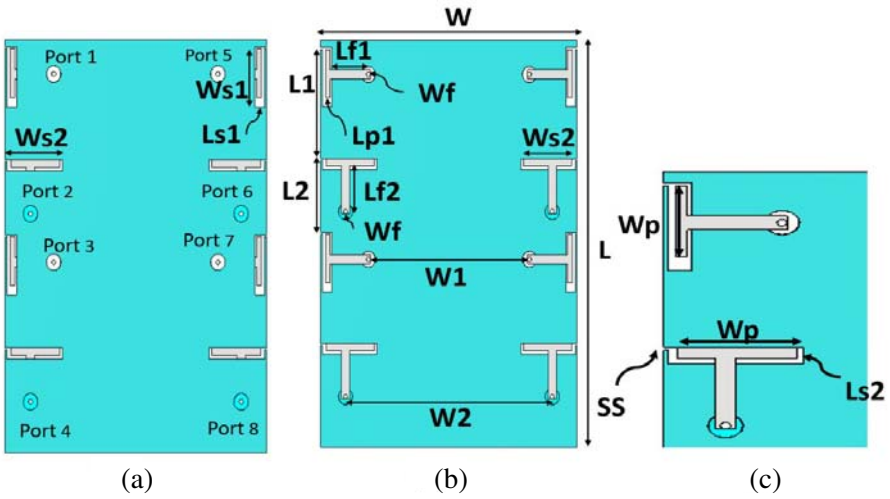

Figure 1. Configuration of the proposed 8-element MIMO antenna, (a) bottom view, (b) top view, (c) a close-up of two orthogonal elements.

Table 1. Optimized parameters of the proposed antenna.

Parameter	Value (mm)	Parameter	Value (mm)
L	110	Wf	2.5
W	90	$Lf1$	12.5
$Ws1$	16	$Lf2$	13
$Ws2$	17.5	$Ls1$	3
$W1$	49	$Ls2$	3
$W2$	64.5	SS	0.5
$Wp1$	15	$L1$	29.5
$Lp1$	1.5	$Lp2$	2
$L2$	20		

dielectric constant of 4.4 and thickness of 0.8 mm. The antenna consists of 8 elements. The configuration of each element consists of a T-shaped radiator that is used to excite an open rectangular slot etched on the ground conductor of the antenna. T-shaped radiators are fed by 50-Ω coaxial connectors. Besides, adjacent elements are positioned orthogonal to each other to mitigate mutual coupling. The size of the open slot controls the resonance frequency of elements. Two different slot sizes are used.

For 1800–2200 MHz band, the open slot size is $Ws1 \times Ls1$ ($0.113\lambda \times 0.02\lambda$). For 2500–2600 MHz band, the used open slot size is $Ws1 \times Ls1$ ($0.106\lambda \times 0.02\lambda$). The distances between ports 1, 2, and 2, 6 are $w1$ and $w2$, respectively. Antennas 1, 3, 5, 7 operate at 1800–2200 MHz band while antennas 2, 4, 6, 8 operate at 2.6 GHz. To gain more insight into the operation of the proposed antenna, the surface current distributions at 2 GHz and 2.6 GHz are shown in Figure 2.

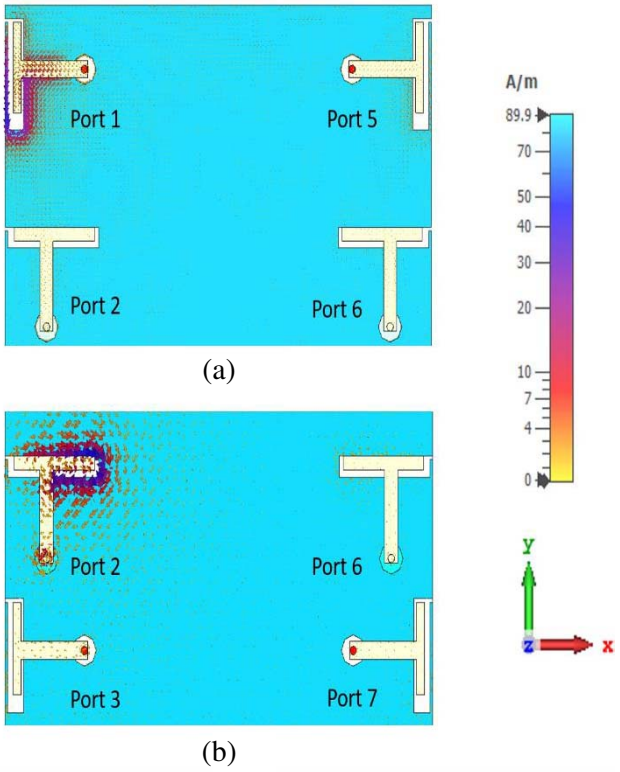

Figure 2. Surface current distributions (A/m), (a) at 2.55 GHz, (b) at 2 GHz.

3. RESULTS AND DISCUSSION

Figure 3 shows the measured and simulated S-parameters of elements 1, 3, 5, and 7. Due to the symmetry of the proposed design, only needed S-parameters are shown. As illustrated in Figure 3, elements 1, 3, 5, and 7 cover LTE 2500 band with isolation less than −14 dB. Antennas 1 and 5 show −6 dB impedance bandwidth of 8% (2.43–2.63 GHz), while antennas 3 and 7 cover a bandwidth of 13% (2.3–2.62 GHz). The S-parameters of elements 2, 4, 6, and 8 are shown in Figure 4. Antennas 2 and 6 exhibit −6 dB impedance bandwidth of 23.5% (1.8–2.28 GHz), while antennas 4 and 8 covers a bandwidth of 27% (1.83–2.4 GHz). It is seen that elements 2, 4, 6, and 8 well cover LTE bands 1/2. The measured isolation is below −10 dB for the elements shown in Figure 4. The discrepancy between measured and simulated results in Figure 4 is due to the FR4 material's impurities. Figure 5 shows photographs of the fabricated prototype design.

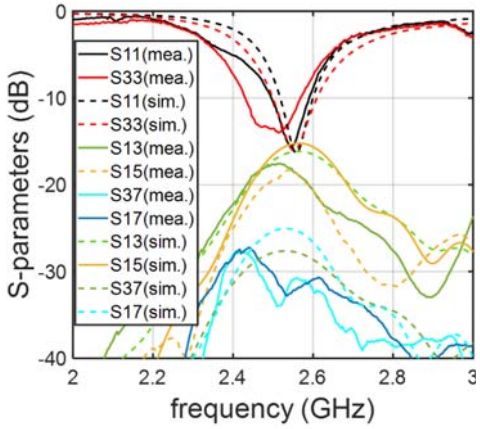

Figure 3. Measured and simulated S-parameters of elements 1 (5), 3 (7) at 2.6 GHz-band.

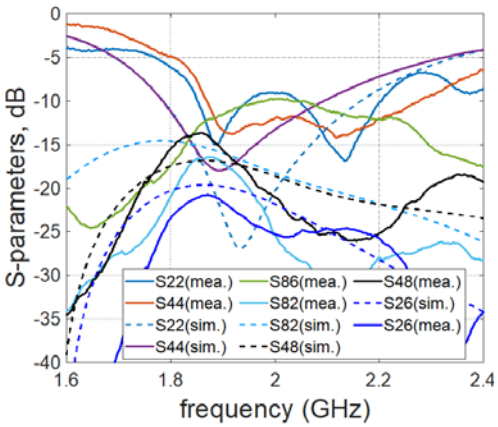

Figure 4. Measured and simulated S-parameters of elements 2 (6), 4 (8) at 1.8–2.2 GHz-band.

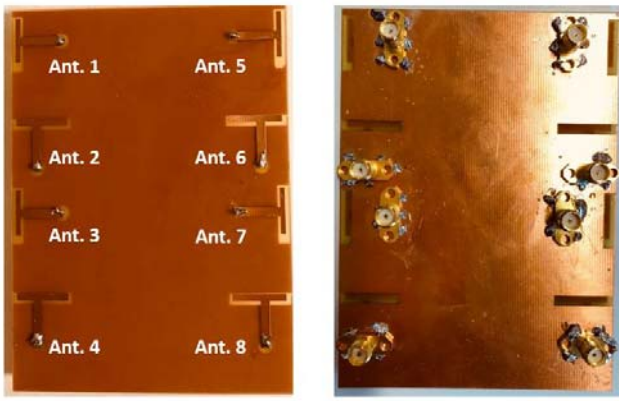

Figure 5. Photographs of the fabricated antenna, (a) front view, (b) back view.

4. RADIATION AND MIMO PERFORMANCES

To gain more insight into the performance of the proposed MIMO antenna system, the total efficiencies of the antenna's elements are calculated as shown in Figure 6. It can be seen that the total efficiency of antennas 1 and 5 is greater than 40%, while it is greater than 44% for antennas 3 and 7 over LTE 2500 band. For LTE 1/2 bands (1.8–2.2 GHz), the total efficiency of antennas 2&6 is greater than 57%, while antennas 4 and 8 show a total efficiency of 52%. To further evaluate the performance of the proposed 8-element MIMO antenna system, the envelope correlation coefficients (ECC) are calculated using [21]:

$$\rho_e = \frac{\oint \left\{ \mathrm{XPR} \cdot E_{\theta 1}(\Omega) E^*_{\theta 2}(\Omega) P_\theta(\Omega) + E_{\emptyset 1}(\Omega) E^*_{\emptyset 2}(\Omega) P_\emptyset(\Omega) \right\} d\Omega}{B1B2}$$

$$B1 = \sqrt{\oint \left\{ \mathrm{XPR} \cdot E_{\theta 1}(\Omega) E^*_{\theta 1}(\Omega) P_\theta(\Omega) + E_{\emptyset 1}(\Omega) E^*_{\emptyset 1}(\Omega) P_\emptyset(\Omega) \right\} d\Omega}$$

$$B2 = \sqrt{\oint \left\{ \mathrm{XPR} \cdot E_{\theta 2}(\Omega) E^*_{\theta 2}(\Omega) P_\theta(\Omega) + E_{\emptyset 2}(\Omega) E^*_{\emptyset 2}(\Omega) P_\emptyset(\Omega) \right\} d\Omega} \quad (1)$$

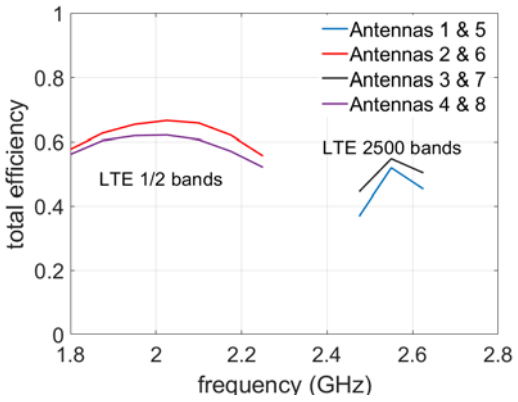

Figure 6. Total efficiencies of the proposed 8-element MIMO antenna system.

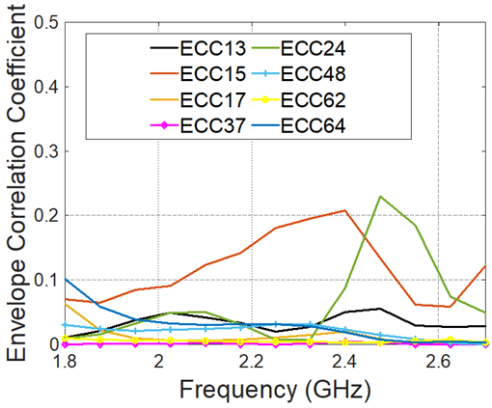

Figure 7. Envelope correlation coefficients.

where XPR is the cross-polarization radiation. For an isotropic environment, XPR $= 1 \cdot E_\theta(\Omega)$ and $E_\emptyset(\Omega)$ are the orthogonal θ- and ϕ-components of the antenna radiation pattern. $P_\theta(\Omega)$ and $P_\emptyset(\Omega)$ are the angular power density functions of the incident wave. The calculated ECC values are less than 0.23 for the operating frequency bands. As illustrated in Figure 7, all ECC values are well below 0.5, which is an approved criterion for MIMO diversity performance.

The simulated and measured normalized radiation patterns of Ant. 1, Ant. 2, Ant. 3, and Ant. 4 in the xz any yz planes are shown in Figure 8. Antennas 1 & 3 patterns are obtained at 2.55 GHz, while antennas 2 & 4 patterns are obtained at 1.9 GHz. Due to the symmetrical structure of the proposed design, the patterns of antennas 5, 6, 7, and 8 are omitted. It can be seen that there is a good agreement in radiation pattern between the simulations and measurements.

Table 2 shows a comparison between the performance of the proposed MIMO antenna and other published MIMO antennas. Compared with other reference antennas, the proposed antenna features a compact size for an 8-element MIMO array as well as good ECC and efficiency performance.

Table 2. Performance comparison between the proposed MIMO antenna and other referenced antennas.

Reference	MIMO order	Bandwidth (GHz) −6 dB	Ground size (mm^2)	Maximum ECC	Efficiency %
Proposed	8	LB: 1.8–2.28 HB: 2.43–2.63	110 × 90	0.16 (LB) 0.23 (HB)	52–62 (LB) 40–58 (HB)
[5]	10	LB: 3.4–3.8 HB: 5.15–5.925	150 × 80	0.15 (LB) 0.05 (HB)	42–65 (LB) 62–82 (HB)
[8]	8	LB: 3.3–4.2 HB: 4.8–5.0	150 × 75	0.1 (LB) 0.12 (HB)	53.8–76 (LB) 62.6–97 (HB)
[12]	8	LB: 3.4–3.6 HB: 4.8–5.1	150 × 70	0.015	61–72 (LB) 64–74 (HB)
[22]	8	LB: 3.54–4.16 HB: 5.10–5.98	150 × 80	0.05	52.2–74.3 (LB) 65.4–82.2 (HB)
[23]	8	LB: 3.6–3.8 HB: 5.15–5.92	150 × 80	0.05	65–73 (LB) 54–74 (HB)

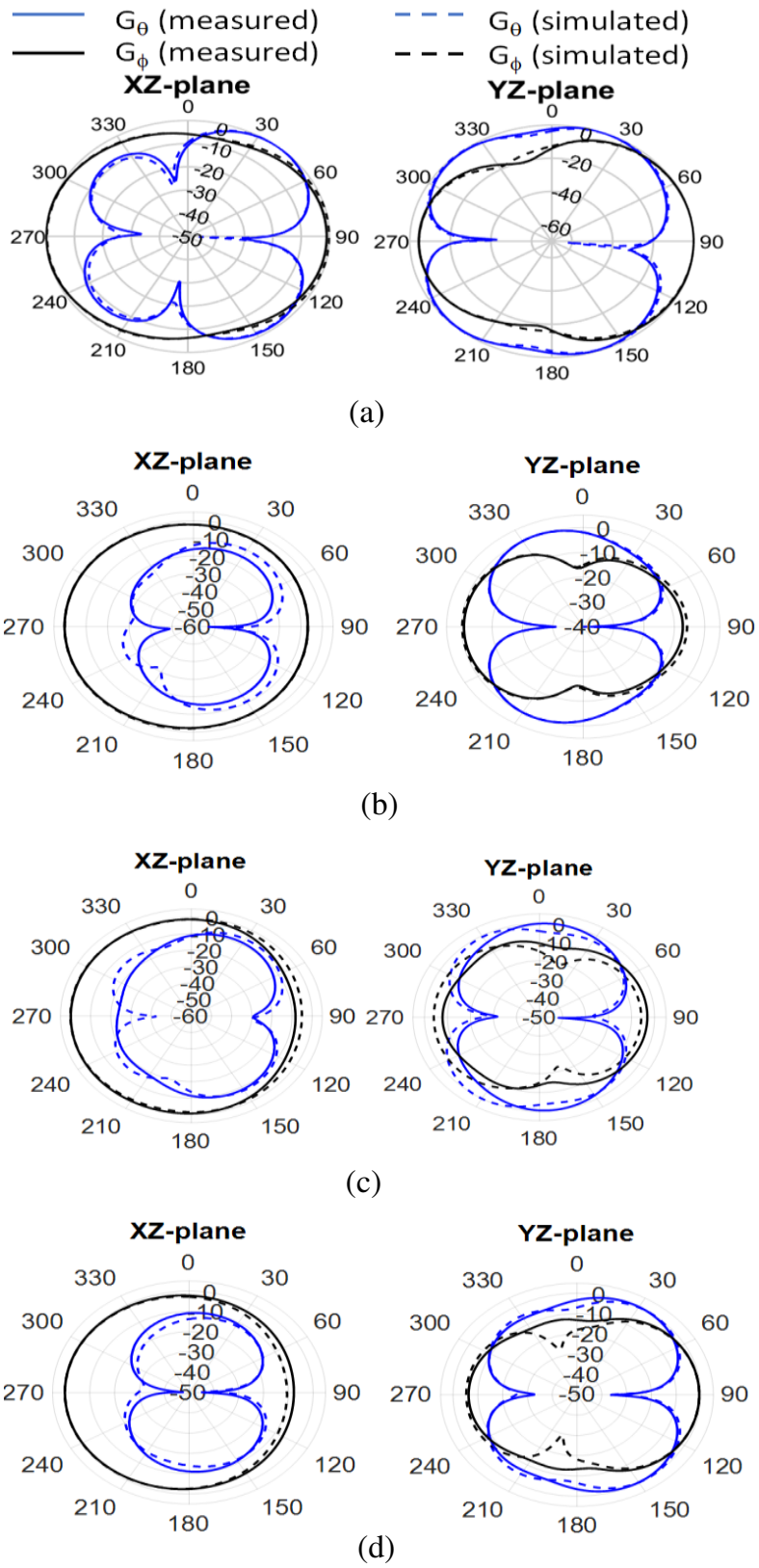

Figure 8. Normalized radiation patterns: (a) Ant. 1 at 2.55 GHz, (b) Ant. 2 at 1.9 GHz, (c) Ant. 3 at 2.55 GHz, (d) Ant. 4 at 1.9 GHz.

5. CONCLUSION

A dual-band 8-element MIMO antenna system that covers the 1800–2200 MHz and 2500–2600 MHz frequency bands is proposed for 5G applications in mobile terminals. The MIMO system employs open slots radiators that are excited by T-shaped microstrip lines. The size of the open slots can mainly determine the operating frequency for each element. The antenna system design was developed using CST Microwave Studio 2021 and verified by testing the fabricated prototype. The testing results show an isolation of less than −10 dB for elements that operate at the 1800–2200 MHz band. Better isolation of less than −14 dB is obtained at the 2500 MHz frequency band. The proposed MIMO system shows good total efficiency and low envelope correlation coefficients. The gain radiation patterns are also analyzed. Based on the simulated and measured results, the antenna is a good candidate for 4/5G MIMO antenna applications.

REFERENCES

1. "Internet of things in the 5G era," *GSMA*, 2019. [Online]. Available: https://www.gsma.com/iot/wp-content/uploads/2019/11/201911-GSMA-IoT-Report-IoT-in-the-5G-Era.pdf. [Accessed: 03-Apr-2020].
2. "Sub 1 GHz spectrum for LTE and 5G," *GSA*, 2019. [Online]. Available: https://gsacom.com/paper/sub-1-ghz-spectrum-for-lte-and-5g/. [Accessed: 03-Apr-2020].
3. Li, Y., C.-Y.-D. Sim, Y. Luo, and G. Yang, "High-isolation 3.5 GHz eight-antenna MIMO array using balanced open-slot antenna element for 5G smartphones," *IEEE Trans. Antennas Propag.*, Vol. 67, No. 6, 3820–3830, Jun. 2019.
4. Zhao, A. and Z. Ren, "Size reduction of self-isolated MIMO antenna system for 5G mobile phone applications," *IEEE Antennas Wirel. Propag. Lett.*, Vol. 18, No. 1, 152–156, Jan. 2019.
5. Li, Y., C.-Y.-D. Sim, Y. Luo, and G. Yang, "Multiband 10-antenna array for sub-6 GHz MIMO applications in 5-G smartphones," *IEEE Access*, Vol. 6, 28041–28053, 2018.
6. Zhao, A. and Z. Ren, "Wideband MIMO antenna systems based on coupled-loop antenna for 5G N77/N78/N79 applications in mobile terminals," *IEEE Access*, Vol. 7, 93761–93771, 2019.
7. Ren, Z. and A. Zhao, "Dual-band MIMO antenna with compact self-decoupled antenna pairs for 5G mobile applications," *IEEE Access*, Vol. 7, 82288–82296, 2019.
8. Cui, L., J. Guo, Y. Liu, and C.-Y.-D. Sim, "An 8-element dual-band MIMO antenna with decoupling stub for 5G smartphone applications," *IEEE Antennas Wirel. Propag. Lett.*, Vol. 18, No. 10, 2095–2099, Oct. 2019.
9. Jiang, W., Y. Cui, B. Liu, W. Hu, and Y. Xi, "A dual-band MIMO antenna with enhanced isolation for 5G smartphone applications," *IEEE Access*, Vol. 7, 112554–112563, 2019.
10. Chattha, H. T., "4-port 2-element MIMO antenna for 5G portable applications," *IEEE Access*, Vol. 7, 96516–96520, 2019.
11. Huang, D., Z. Du, and Y. Wang, "A quad-antenna system for 4G/5G/GPS metal frame mobile phones," *IEEE Antennas Wirel. Propag. Lett.*, Vol. 18, No. 8, 1586–1590, Aug. 2019.
12. Wei, G. and Q. Feng, "Dual-band MIMO antenna array for compact 5G smartphones," *Progress In Electromagnetics Research C*, Vol. 99, 157–165, 2020.
13. Wang, H., R. Zhang, Y. Luo, and G. Yang, "Compact eight-element antenna array for triple-band MIMO operation in 5G mobile terminals," *IEEE Access*, Vol. 8, 19433–19449, 2020.
14. Parchin, N. O., et al., "Eight-element dual-polarized MIMO slot antenna system for 5G smartphone applications," *IEEE Access*, Vol. 7, 15612–15622, 2019.
15. Sun, L., H. Feng, Y. Li, and Z. Zhang, "Compact 5G MIMO mobile phone antennas with tightly arranged orthogonal-mode pairs," *IEEE Trans. Antennas Propag.*, Vol. 66, No. 11, 6364–6369, Nov. 2018.
16. Ren, Z., S. Wu, and A. Zhao, "Triple band MIMO antenna system for 5G mobile terminals," *2019 International Workshop on Antenna Technology (iWAT)*, 163–165, 2019.

17. Hussain, R., A. T. Alreshaid, S. K. Podilchak, and M. S. Sharawi, "Compact 4G MIMO antenna integrated with a 5G array for current and future mobile handsets," *IET Microwaves, Antennas Propag.*, Vol. 11, No. 2, 271–279, Jan. 2017.
18. Ban, Y. L., C. Li, C. Y. D. Sim, G. Wu, and K. L. Wong, "4G/5G multiple antennas for future multi-mode smartphone applications," *IEEE Access*, 2016.
19. Sharawi, M. S., M. Ikram, and A. Shamim, "A two concentric slot loop based connected array MIMO antenna system for 4G/5G terminals," *IEEE Trans. Antennas Propag.*, Vol. 65, No. 12, 6679–6686, Dec. 2017.
20. "CST studio suite," *Dassault Systèmes*, 2019. [Online]. Available: www.cst.com. [Accessed: 03-Apr-2020].
21. Stein, S., "On cross coupling in multiple-beam antennas," *IRE Trans. Antennas Propag.*, Vol. 10, No. 5, 548–557, Sep. 1962.
22. Aziz, H. S. and D. K. Naji, "Printed 5G MIMO antenna arrays in smartphone handset for LTE bands 42/43/46 applications," *Progress In Electromagnetics Research M*, Vol. 90, 167–184, 2020.
23. H. S. Aziz and D. K. Naji, "Compact dual-band MIMO antenna system for LTE smartphone applications," *Progress In Electromagnetics Research C*, Vol. 102, 13–30, 2020.